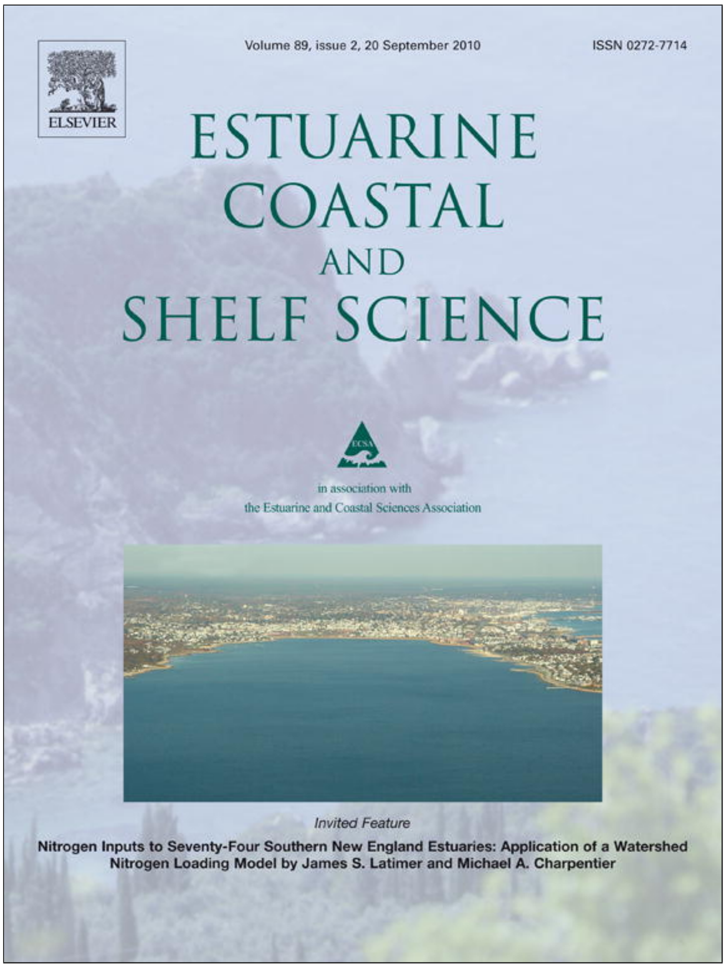
Volume 89, issue 2, 20 September 2010
ISSN 0272-7714
ELSEVIER
ESTUARINE
COASTAL
AND
SHELF SCIENCE
in association with
the Estuarine and Coastal Sciences Association
Invited Feature
Nitrogen Inputs to Seventy-Four Southern New England Estuaries: Application of a Watershed Nitrogen Loading Model by James S. Latimer and Michael A. Charpentier

Estuarine, Coastal and Shelf Science 89 (2010) 154–162

Contents lists available at ScienceDirect

Estuarine, Coastal and Shelf Science

journal homepage: www.elsevier.com/locate/ecss

Importance of wave-induced bed liquefaction in the fine sediment budget of Cleveland Bay, Great Barrier Reef

J. Lambrechts [a,*], C. Humphrey [b], L. McKinna [c], O. Gourge [a], K.E. Fabricius [b], A.J. Mehta [d], S. Lewis [e], E. Wolanski [b,e]

[a] Centre for Systems Engineering and Applied Mechanics, Université catholique de Louvain, B-1348 Louvain-la-Neuve, Belgium
[b] Australian Institute of Marine Science, Townsville, Queensland 4810, Australia
[c] School of Engineering and Physical Sciences, James Cook University, Townsville, Queensland 4811, Australia
[d] Department of Civil and Coastal Engineering, 365 Weil Hall, University of Florida, Gainesville, FL 32611, USA
[e] Australian Centre for Tropical Freshwater Research, James Cook University, Townsville, Queensland 4811, Australia

ARTICLE INFO

Article history:
Received 18 March 2010
Accepted 12 June 2010
Available online 19 June 2010

Keywords:
fine sediment
waves
erosion
deposition
model
coral
Great Barrier Reef

ABSTRACT

Data from a three-year long field study of fine sediment dynamics in Cleveland Bay show that wave-induced liquefaction of the fine sediment bed on the seafloor in shallow water was the main process causing bed erosion under small waves during tradewinds, and that shear-induced erosion prevailed during cyclonic conditions. These data were used to verify a model of fine sediment dynamics that calculates sediment resuspension by both excess shear stress and wave-induced liquefaction of the bed. For present land-use conditions, the amount of riverine sediments settling on the bay may exceed by 50–75% the amount of sediment exported from the bay. Sediment is thus accumulating in the bay on an annual basis, which in turn may degrade the fringing coral reefs. For those years when a tropical cyclone impacted the bay there may be a net sediment outflow from the bay. During the dry, tradewind season, fine sediment was progressively winnowed out of the shallow, reefal waters.

1. Introduction

Engineers have pioneered the research on the dynamics of marine sediment transport and have proposed a number of conventional formulae for erosion and settling rates that are relied on for the last few decades (Dyer, 1986; Partheniades, 1986; Winterwerp and van Kesteren, 2004). This reliance has proven to be a fundamental obstacle to progress in simulating the transport of marine sediments because these formulae neglect the role of wave-induced pore-pressure variations in liquefying the sediments, thus enhancing the bed erosion (Maa and Mehta, 1987; Aldridge and Rees, 1997). This paper proposes a parameterisation of this effect.

Commonly in the literature (Dyer, 1986), the erosion flux E is parameterised by,

$$E = \{M_e((u_b/u_c)^n - 1), \quad \text{if } u_b > u_c, \quad \text{if } u_b < u_c\} \tag{1}$$

where M_e is a parameter that characterises the bottom sediment properties including the effect of the biology on its erodibility, u_c is the threshold velocity for erosion, and n is a constant. Laboratory studies suggest $n = 2–4$, while field experiments suggest that $n = 4–6$ (Wolanski et al., 1995; Johansen et al., 1997; Wolanski and Spagnol, 2003). A reason for this discrepancy may be the biology that laboratory experiments cannot reproduce, namely the competing influences of algae that tend to make the mud less erodible and of bioturbation that makes the mud more erodible (Wolanski, 2007; Maerz and Wirtz, 2009; Andersen et al., 2010).

In the presence of waves, it is unclear how to apply Eq. (1) because waves enhance mud erosion both by increasing the bottom shear stress and by liquefying the bottom mud by generating excess pore pressure in the substrate; the fluid mud thus formed is readily brought up in suspension by tidal currents of speed $u \ll u_c$, thus invalidating Eq. (1) (Maa and Mehta, 1987; Aldridge and Rees, 1997). In mathematical models for E, excess pore-pressure effects are commonly neglected, so that bed erosion is assumed to result from shear stresses only; thus M_e is assumed to be a constant and u_b is calculated from the combined shear stresses of the currents and the wave orbital velocity (Sheng and Lick, 1979; Soulsby et al., 1993). However bed fluidisation always occur under waves, even if the waves are small. Thus Eq. (2) should be modified to parameterise wave-induced liquefaction. Eq. (2) could

* Corresponding author.
E-mail address: jonathan.lambrechts@uclouvain.be (J. Lambrechts).

0272-7714/$ – see front matter
doi:10.1016/j.ecss.2010.06.009

theoretically be modified by assuming smaller values of u_c in the presence of waves. However this would over-simplify the problem because several studies have found that waves also influence M_e (Wolanski et al., 1995; Rodriguez and Mehta, 2000; Foda and Huang, 2001; Wolanski and Spagnol, 2003),

$$M_e \propto H_s^3 \tag{2}$$

or

$$M_e \propto \{(H_s - h_0), \quad \text{if } H_s > h_0; \; 0, \quad \text{if } H_s < h_0\} \tag{3}$$

or

$$M_e \propto \left\{(H_s - h_0)^3 \quad \text{if } H_s > h_0; \; 0, \quad \text{if } H_s < h_0\right\} \tag{4}$$

where H_s is the significant wave height and h_0 is a critical wave height, which is the smallest height of the waves impacting the bottom sediment. No published study has quantified how to modify both u_c and M_e to include wave-induced liquefaction in Eq. (1).

This paper addresses this issue in order to estimate the net budget of fine sediment in Cleveland Bay, Australia (Fig. 1a). Rates of sediment transport and sedimentation in these waters are unknown, though a wind-driven northward littoral sediment drift has been inferred from longshore variation of sediment composition and texture along the 10 m isobath (Lambeck and Woolfe, 2000). The bay is impacted by the discharge of two local, seasonal rivers, namely the Ross River and Alligator Creek with catchment areas of 998 km^2 and 265 km^2, respectively. Both catchments, particularly the catchment of the Ross River, are heavily impacted by human developments and sediment and nutrient exports have increased several folds since European settlement in the region (c. 1860s) (Furnas, 2003). The bay may also receive fine sediment from the Burdekin River; the mouth is located about 100 km to the south; that river is one of the largest in Australia with a 130,126 km^2 catchment; it is used predominantly for grazing and it discharges 3.77 10^6 t y^{-1} of fine sediment and 8633 and 1695 t y^{-1} of nitrogen and phosphorus, respectively (Furnas, 2003). The sediment flux from the Burdekin River has increased by ~4 fold since European settlement in the catchment (Furnas, 2003).

Published studies of sediment dynamics in this bay were focused in the central and eastern area, far from the corals fringing Magnetic Island; this is the area with the deepest waters and where mud dredged to enable navigation was dumped for the past five decades over a sandy mud substrate. The studies revealed that the bottom mud was stable, being resuspended only under rare swell and storm events, while its distribution has been markedly affected by the dumping of dredge spoil (Wolanski et al., 1992; Carter et al., 1993; Lou and Ridd, 1997).

This paper is divided in three sections. Firstly, the results of a three-year long field study recording mud dynamics in Cleveland Bay are described; they show no resuspension during calm weather conditions, minor resuspension under small waves and small tidal currents in shallow waters during the tradewinds, and a greater but still moderate resuspension under cyclonic conditions. Secondly, resuspension dynamics are modelled; it is shown that Eqs. (1)–(5) are unable to explain the observations; these equations were modified to parameterise the wave-induced pore pressure build-up in the substrate, yielding a new, semi-empirical formula for mud erosion by both excess shear stresses and excess wave-induced pore pressure. Thirdly, the net fine sediment budget is examined for Cleveland Bay which suggests that land-use in the adjoining river catchment results in the accumulation of riverine mud in reefal waters, which in turn may degrade the fringing coral reefs.

2. Methods

2.1. Field studies

A self-cleaning Analite nephelometer was deployed on September 16, 2005, at site 1 near Magnetic Island (Fig. 1 and Table 1). Two other Analite nephelometers were deployed at sites 2 and 3 on 13th September 2007. Data were obtained at 10 min intervals until the end of January 2009. Field trips were conducted on a 3- to 6-weekly basis to download data and service the instruments (Table 1). The turbidity readings were converted to SSC using a calibration curve, estimated using local mud, for each instrument.

Wind speed and direction data at 30 min intervals at site 4 were obtained from the Australian Institute of Marine Science. Significant wave height and period data at 30 min intervals at site 5 were obtained from the Queensland Department of Environment and Resource Management. Current meter data were available at sites 6–8 from Wolanski et al. (1992). Tide data from the port of Townsville at 10 min intervals were obtained from Maritime Safety Queensland. Data on the timing and location of dredging operations along the shipping channel were provided by the Townsville Port Authority.

Height data for the Ross River at Aplins Weir were obtained from the Commonwealth Bureau of Meteorology and converted to discharge using a rating curve. The Ross River at Aplins Weir was sampled for SSC and these data were combined with the river discharge data to calculate the fine sediment discharge (Lewis et al., 2008). The flood plume in Cleveland Bay from the Ross River discharge was sampled for surface salinity and SSC in February 2007 (Liessmann et al., 2007). The Burdekin River flood plume at the mouth of Cleveland Bay was also similarly sampled in 2007 and 2008.

In situ microphotographs of sediment flocs in suspension were obtained in January 2007 using the method of Ayukai and Wolanski (1997).

To map the SCC distribution within Cleveland Bay during tradewinds, ocean colour satellite imagery was used. The normalised water-leaving radiance (nLw) of band 1 of the Moderate Resolution Imaging Spectroradiometer Aqua (MODIS-Aqua) 1 centred at 645 nm was used. MODIS band 1 provides a 250m pixel resolution and recent studies have shown it is useful in observing SSC in coastal waters (Miller and Mckee, 2004; Chen et al., 2007; Lahet and Stramski, 2010; Zhang et al., 2010). MODIS raw level-0 data were acquired from NASA's Ocean Color website and processed to a calibrated, geophysical, level-2 product of nLw(645) using SeaWiFS Data Analysis System (SeaDAS version 5.4; Baith et al., 2001). The atmospheric correction used over the turbid, coastal waters of Cleveland Bay was the near-infrared, shortwave infrared (NIR-SWIR) switching algorithm (Wang and Shi, 2007). There is currently no region-specific SSC algorithm for Cleveland Bay. Therefore MODIS nLw(645) was used as a proxy for SSC spatial distribution within the bay.

2.2. Numerical modelling

For the oceanography, the non-structured grid numerical model SLIM was used (Lambrechts et al., 2008). The model domain (not shown) covers the whole 1600 km long Great Barrier Reef (GBR). The near-field grid is shown in Fig. 1b; the horizontal resolution varies between 100 m in the area of the Port of Townsville and 10 km far away from Cleveland Bay. The model forcings were the East Australian Current, the wind, the tides, and the Ross River discharge. This model was used to drive a fine sediment dynamics model that relied initially on Eqs. (1)–(5) for calculating deposition and erosion; these equations were then modified to calculate bed erosion due to

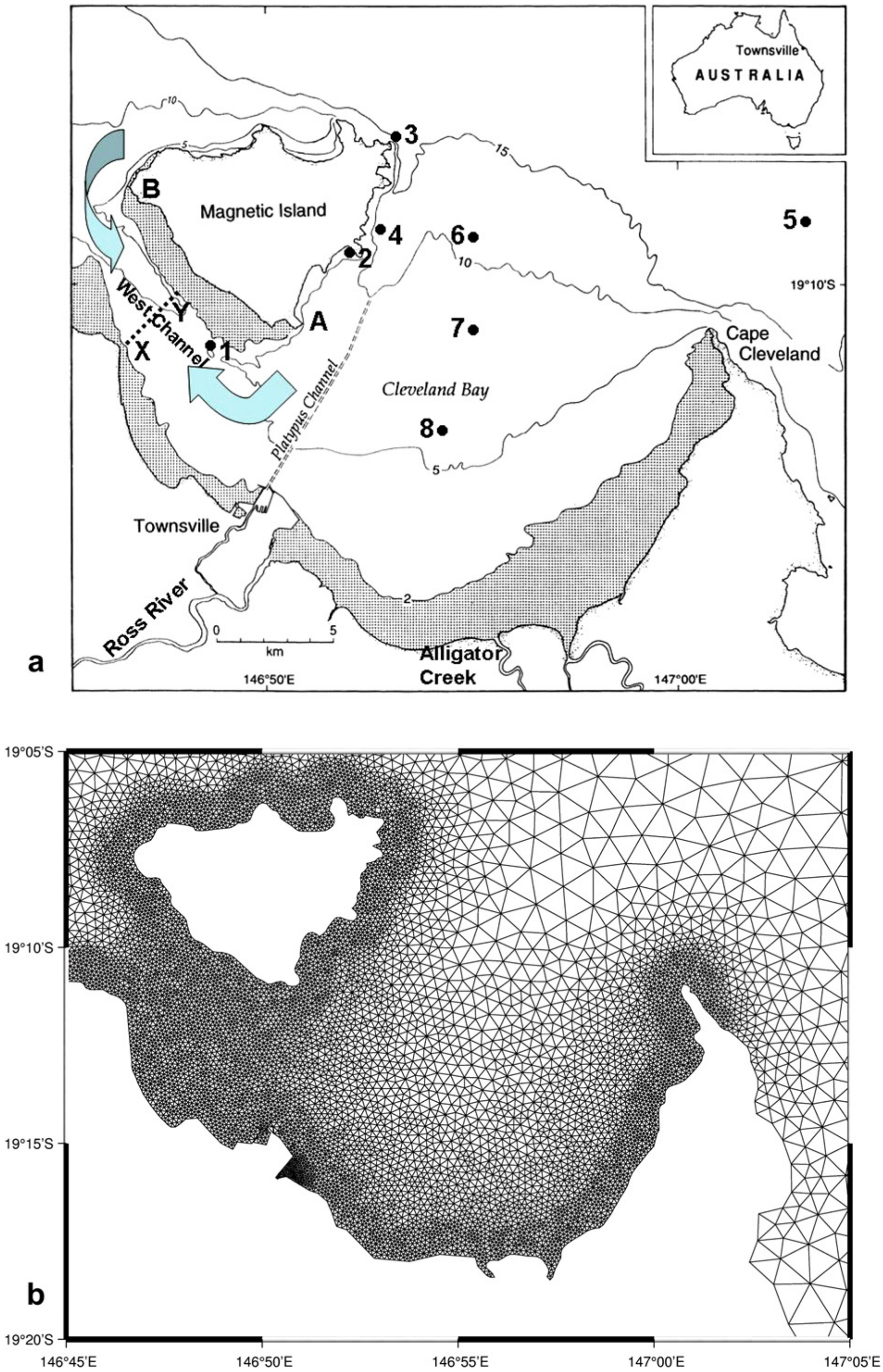

Fig. 1. (a) A chart of Cleveland Bay showing the location of the SSC measurements at sites 1 (Middle Reef), site 2 (Geoffrey Bay) and site 3 (Orchard Rock), the weather station at site 4, the wave rider buoy at site 5, and the current meter moorings at sites 6–8. Depth is in meters. The arrows show the flood tidal currents entering West Channel and converging at the stagnation line *X*–*Y* during calm weather. The ebb tidal currents during calm weather diverge from the same line. A = Hawkings Point, B = West Point, C = Ross River, D = Alligator Creek. Platypus Channel is a dredged navigation channel, West Channel is natural. (b) The near-field grid of the oceanographic model.

both, the excess shear stress and the excess wave-induced pore pressure in the substrate, as explained below in the results.

3. Results

3.1. Fine sediment dynamics in the dry season

The dry season is the tradewind season, which typically lasts from April to November. Fig. 2a shows that resuspension at site 1 and at the other two sites (not shown) occurred only in the presence of waves and that the tidal currents were too small in the absence of waves to resuspend the bottom sediment. The 0D model for wave-induced resuspension using Eq. (4) and assuming $h_0 = 0.2$ m predicted satisfactorily the timing and the peak SSC values of the resuspension events. A few events at the end of the dry season, labelled 1, 2, and 3 in Fig. 2A, were overpredicted by the 0D model. As is shown in Fig. 2B, during each event the mud was resuspended during periods of maximum significant wave height

Table 1
The Nephelometer mooring sites around Magnetic Island.

Site	Name	Location	Characteristics
1	Middle Reef	19° 11.972 S 146° 49.097 E	Logger was ~0.5 m above the seafloor composed of soft, fine sediment. Maximum depth ~4.9 m below LAT
2	Geoffrey Bay	19° 09.29 0S 146° 52.111 E	Logger was located on the lower end of the reef slope, ~0.5 m above the seafloor composed of ~50% hard substratum and 50% coral rubble Maximum depth ~5.5 m below LAT
3	Orchard Rocks	19° 06.655 S 146° 52.807 E	Logger was located on the island slope ~0.5 m above the seafloor that was a combination of coral outcrops, granitic bed rock and fine sediment. Maximum depth ~6.4 m below LAT

and wave period, and also varied with the tide. The 0D model overpredicted the duration of the resuspension events.

Water-leaving radiance in MODIS images were used to visualise the near-surface SSC distribution during the tradewind season. These images show (Fig. 3) a near-surface SSC that was maximum inshore and decreased seaward, forming a turbid coastal boundary layer; within this layer the SSC distribution was patchy, with highest values near headlands and SSC values declining seawards from Site 1 to Sites 2 and 3. A similar pattern was observed in other images (not shown). The Zhang et al. (2010) quantitative SSC MODIS algorithm for the temperate East China and Yellow Seas was examined as a method to retrieve SSC; however, the derived values were an order of magnitude smaller than in situ observations (not shown).

3.2. Fine sediment dynamics in cyclonic conditions

Data were collected during January 2009 under Tropical Cyclone Hamish, with H_s peaking at 3.6 m^{-1} and T_s of 8 s. The SSC values generally decreased seaward, varied weakly with the tide, and showed a long period of weakly-varying, quasi-steady SSC during the storm and for about a day after the storm (Fig. 4a). SSC values exceeded 200 mg l^{-1} for about 8 and 30 h during this storm at Middle Reef and Geoffrey Bay, respectively.

3.3. Fine sediment dynamics during river floods

The February 2007 Ross River flood plume water moved alongshore northward past Middle Reef but did not reach Magnetic Island. The plume data from the Ross River showed that near-surface SSC was 100 mg l^{-1} near the mouth at salinity = 2, and ~4 mg l^{-1} at site 1 (Middle Reef) where the salinity was 20. At the Middle Reef mooring site the average SSC at 4.4 m depth during the peak of the flood was about 14 mg l^{-1}, with peak values of 24 mg l^{-1}.

The 2006/07 and 2007/08 plume from the Burdekin River at the mouth of Cleveland Bay had salinity and SSC of 25–27 and 3–7 mg l^{-1}, respectively and the plumes lasted typically 7 days.

3.4. Modelling

The oceanographic model reproduced well (not shown) the current meter observations at the sites 6–8. During calm weather conditions the flood tidal currents entered Cleveland Bay both east and west of Magnetic Island at peak speeds of ~0.2 m s^{-1}. These currents converged towards a stagnation line in West Channel (see Fig. 1a). The currents diverged from that line at ebb tide. During tradewinds this stagnation line shifted westward to West Point. During Tropical Cyclone Hamish the currents in West Channel did not reverse direction with the tide and were alongshore northward at a velocity peaking at 0.7 m s^{-1} (not shown).

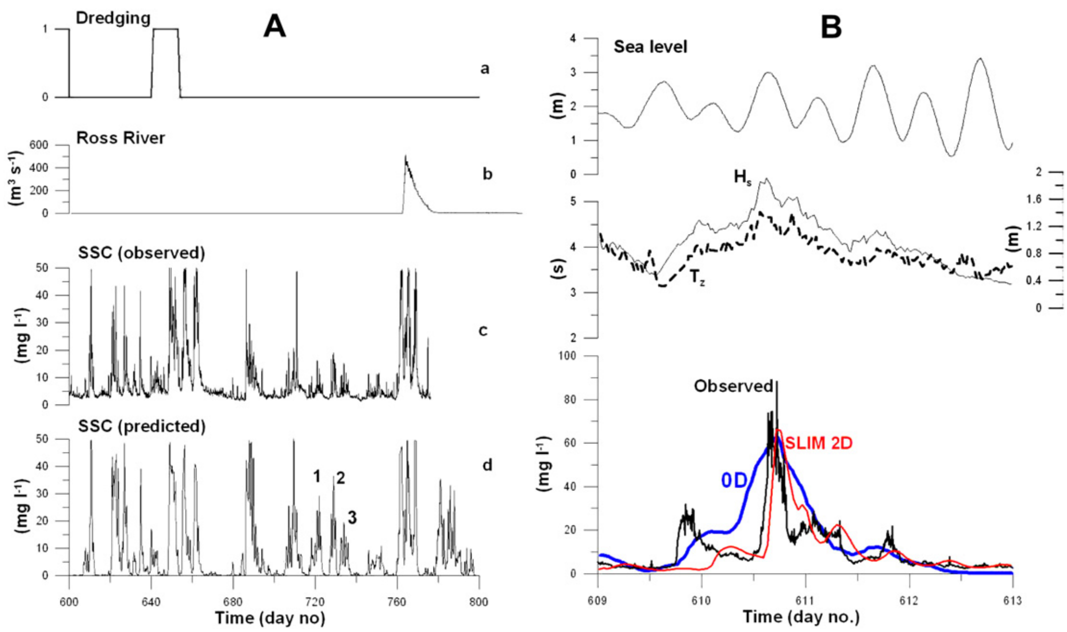

Fig. 2. (A) Time-series plot of (a) dredging activities (1 = dredging; 0 = no dredging), (b) Ross River discharge, and (c) observed and (d) predicted SSC at Middle Reef. 1, 2, and 3 refer to events nearer the end of the dry season where high SSC values were predicted but not observed. The Ross River discharge lasted only about 10 days during the wet season. (B) Time-series plot of the sea level, significant wave height H_s and period T_z, observed SSC, and SSC predicted by the 0D and the SLIM 2D models during the trade wind event of day 609–612. Time is in day number from 1 January 2005.

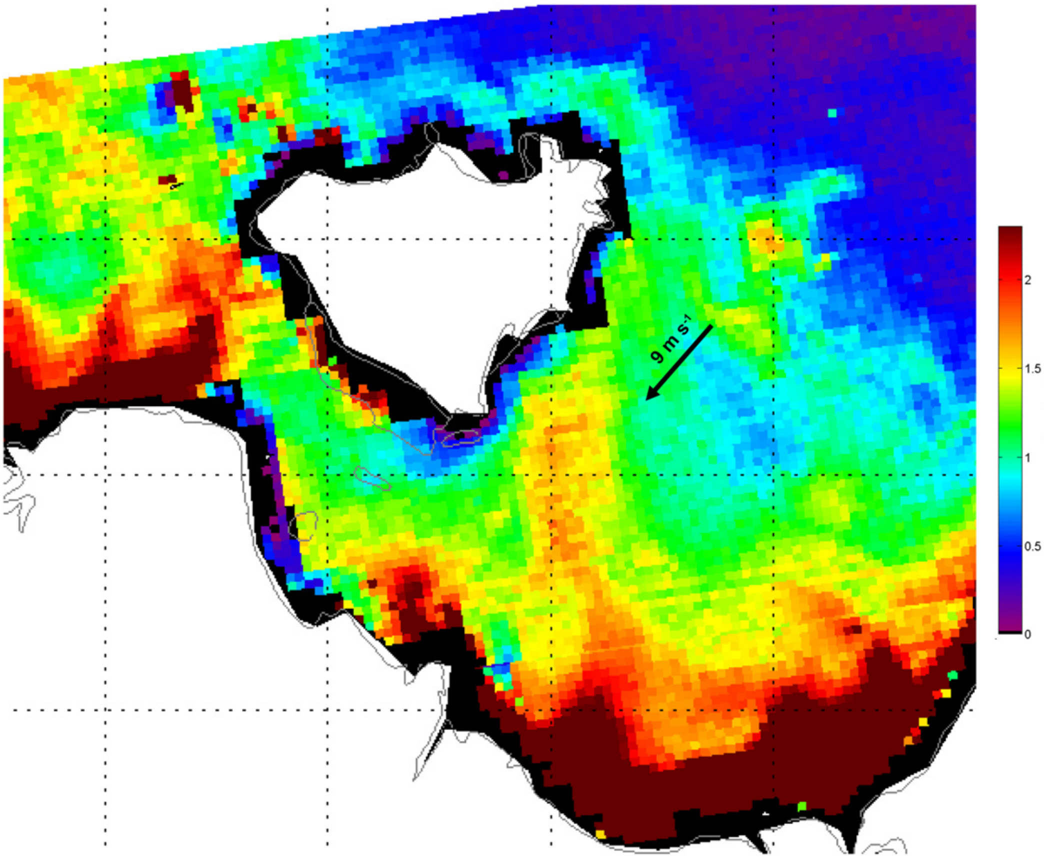

Fig. 3. Distribution of the MODIS normalised water-leaving radiance 645 nm, at horizontal resolution of 250 m, on July 27, 2009, i.e. in the dry season, at 1350 h, near slack high tide. The black arrows show the wind speed and direction. The black bands along the coast are pixels that are suspected of being contaminated by the land signal.

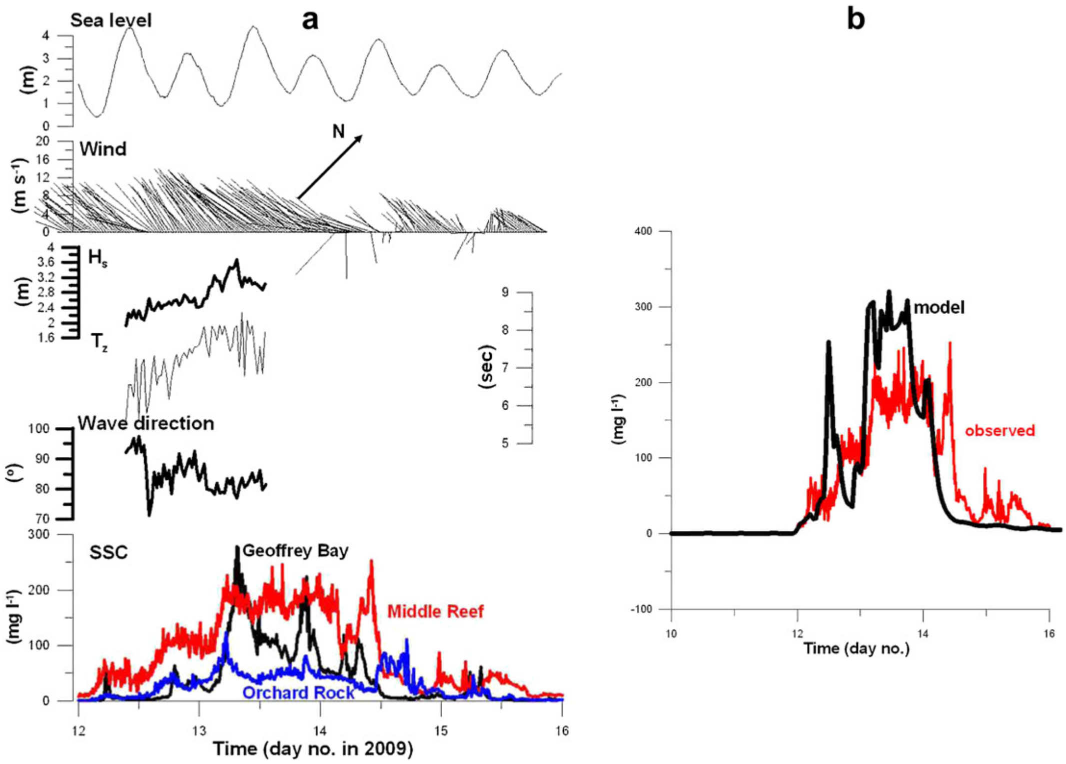

Fig. 4. (a) Time-series plot for the January 2009 storm of the sea level, the wind (using the oceanographic convention), the significant wave height H_s, wave period T_z, and wave direction, and the suspended sediment concentration (SSC) at the mooring sites. (b) Time-series plot of the observed and predicted SSC at Middle Reef. Time is in day number in 2009.

These data were used to calibrate the fine sediment dynamics model for wave-dominated muddy, shallow waters. Because the suspended sediment was in the flocculation-enhanced settling range and because the flocs were of similar size and shape as in the tropical Fly River estuary and King Sound (not shown), the dependence of w_s (m s^{-1}) on C (mg l^{-1}) was taken from field observation (Wolanski et al., 1995; Wolanski and Spagnol, 2003),

$$w_s = 0.00001C \quad (5)$$

Eq. (5) is only valid in the enhanced settling range when $C < 3000$ mg l^{-1}, which is the case in Cleveland Bay. The settling flux, D, of the mud in suspension was then calculated following Einstein and Krone (1962),

$$D = \left\{Cw_s\left(1-(u_b/u_d)^2\right), \quad \text{if } u_b < u_d; \; 0, \quad \text{if } u_b > u_d\right\} \quad (6)$$

where C is the suspended sediment concentration (SSC), w_s is the settling velocity, u_b is the near-bottom velocity, and u_d is the threshold velocity for settling.

Using Eqs. (2)–(5) the model was unable to reproduce with the same parameters all the observations during calm weather, during tradewinds, and during cyclonic conditions. Indeed in Cleveland Bay, u_c is about 0.3 m s^{-1} (Wolanski et al., 1992; Lou and Ridd, 1997). During tradewinds, the largest waves had H_s ~0.8 m and T_s ~4 s (Fig. 2B); in depth of 4 m these waves generated only a small additional shear stress so that in Eq. (1) u ~0.2 m s^{-1} $<u_c$, so that no bed erosion is predicted, which is contrary to the observations. One could presumably force Eq. (1) to predict erosion by decreasing u_c by 45% to reproduce the observations, on the assumption that the bed was weakened by wave-induced, excess pore-pressure. If such assumption were correct, then the decrease of u_c would be proportional to H_s. However such an assumption would become meaningless under Tropical Cyclone Hamish when H_s ~3.2 m it would result u_c ~0; the resulting model then overpredicted by a factor of 100 the observed SSC (not shown). Eq. (1) thus appears unable to explain all the observations. A new method was thus necessary to calculate bed erosion due to excess shear stress and wave-induced excess pore pressure. Accordingly, the resuspension model was modified to explicitly parameterise wave-induced pore water pressure build-up. The erosion flux (E) was modelled as,

$$E = E_1 + E_2 \quad (7)$$

where E_1 is the erosion due to wave-induced pore pressure build-up and resulting liquefaction of the bed which can then be eroded without the need for $u > u_c$, and E_2 is obtained from an expression of the form of Eq. (1) for erosion by excess shear stress without wave-induced liquefaction of the bed,

$$E_1 = A_1 H_s^3 F(\omega, H) \quad (8)$$

$$E_2 = \left\{A_2\left((|V|/u_c)^n - 1\right), \quad \text{if } |V| > u_c; \; 0 \quad \text{if} |V| < u_c\right\} \quad (9)$$

where F is a function of wave frequency ω and water depth H, $|V|$ is the water speed averaged over at least 1 min (i.e. not including the wave orbital velocities), and A_1 and A_2 are empirical constants that depend only on the characteristics of the fine sediment on the seafloor. The assumption of third power in Eq. (8) is supported by the field data that show that the SSC was proportional to the third power of the wind speed (Fig. 5) and that during tradewinds H_s was proportional to wind speed (not shown). Pore-pressure build-up was assumed proportional to wave-induced pressure fluctuations on the seafloor, so that (Kuo and Chiu, 1994; Tsai et al., 2005),

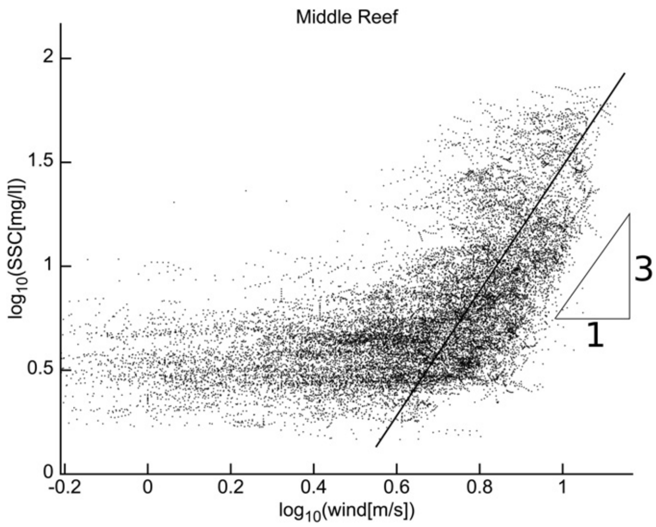

Fig. 5. A double-log scatter plot of suspended sediment concentration at site 1 versus the wind speed during 2006–2008.

$$F = \exp\left(-0.905\omega^2 H/g - 0.027\right) \quad (10)$$

where g is the acceleration due to gravity.

The model was successful in reproducing the SSC observations at Middle Reef during tradewinds (Fig. 2b) and during cyclonic conditions (Fig. 4b), as well as correctly predicting no resuspension during calm weather conditions.

4. Discussion

The fine sediment in Cleveland Bay was mobile (in large quantity) only during a number of discrete events, namely during river floods, tradewinds, and cyclones. During calm weather conditions the bottom sediment was not resuspended. It was resuspended during strong tradewinds but the waves were small and, from linear wave theory it was found that these waves only marginally increased the bottom shear stress. The classical formula (e.g. Dyer, 1986) for bed erosion based solely on the excess shear stress failed in Cleveland Bay. It is argued that this formula needs to be modified to parameterise wave-induced excess pore pressure build-up, so that the bed erodes only by wave-induced bed liquefaction during strong tradewinds, and by both excess shear stress and wave-induced bed liquefaction under cyclonic conditions. Such a formula is proposed as Eqs. (7)–(10) that satisfactorily reproduce the observations across a wide range of oceanographic conditions without changing the calibrated values of the empirical coefficients A_1 and A_2.

The SSC distribution shows patchiness in the turbid coastal boundary layer. The reason for this patchiness may be the headland eddies that are predicted to have a diameter of 500–2000 m. Those eddies create patches of muddy waters that are advected away from the coast when the currents reverse direction with the tides. Based on the data and the model, the following fine sediment budget for Cleveland Bay is proposed and is summarised in Fig. 6. The Ross River discharged 26,500 t y^{-1} and 14,500 t y^{-1} of fine sediment in Cleveland Bay in 2007 and 2008, respectively (Bainbridge et al., 2007); taking into account the additional contribution from Alligator Creek, the average fine sediment discharge in Cleveland Bay was 25,900 t y^{-1}. During tradewinds the SLIM model suggests that fine sediment in suspension was exported alongshore northward through West Channel at a rate of ~860 t d^{-1}. As there are typically 25 days of strong tradewinds per year, the annual export was ~21,500 t y^{-1} of fine sediment. The

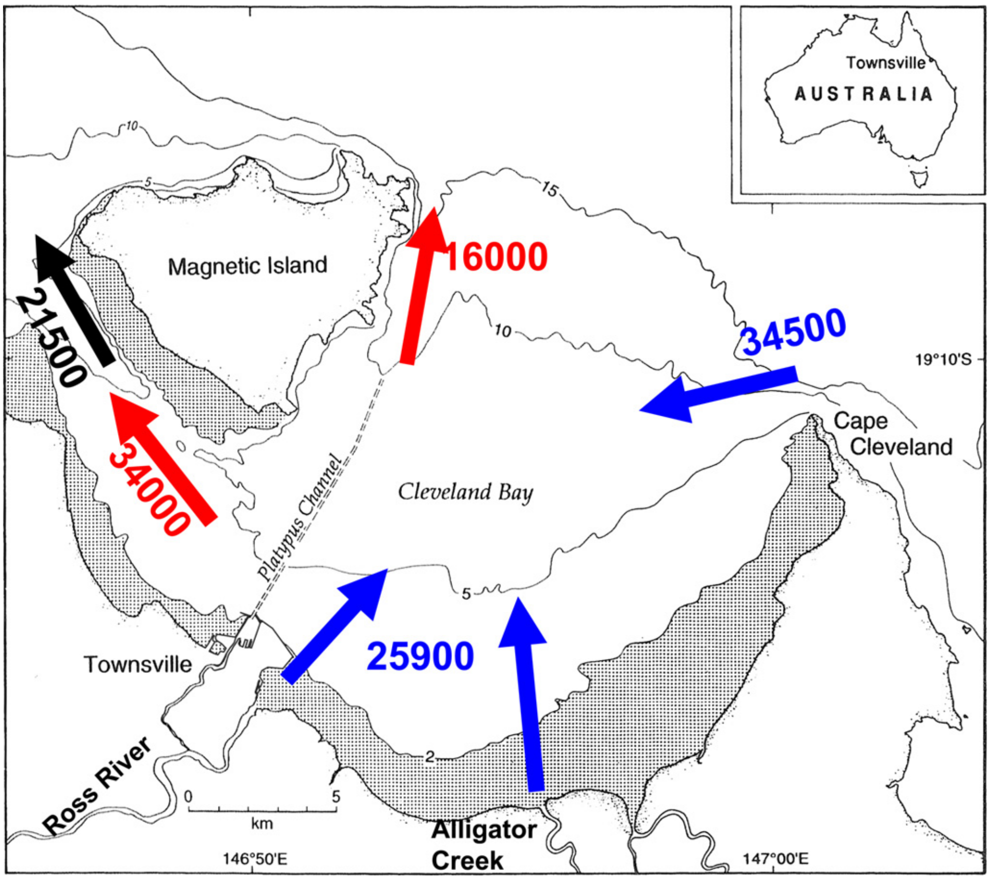

Fig. 6. Estimates of the fluxes ($t\,y^{-1}$) of fine sediment (blue arrows) entering Cleveland Bay from land runoff, the Burdekin River plume and strong trade winds, and (black arrow) leaving Cleveland Bay under tradewinds and (red arrows) under a tropical cyclone. (For interpretation of the references to colour in this figure legend, the reader is referred to the web version of this article).

model also suggests that tropical cyclone Hamish exported ~34,000 t of fine sediment from Cleveland Bay through the West Channel and ~16,000 t seaward along the east coast of Magnetic Island. Also, fine sediment from the Burdekin River may enter Cleveland Bay in the river plume that travels northward longshore in coastal waters and lasts typically 7 days y^{-1} (King et al., 2001). The Burdekin River plume is not visible in Fig. 3 because the plume only occurs in the wet season and the image was obtained in the dry season. In addition, Burdekin River sediment deposited in coastal waters between Cleveland Bay and the mouth of the Burdekin River is resuspended during 25 days of strong tradewinds and enters Cleveland Bay with a SSC of 3 mg l^{-1} (Lewis et al., 2008). Burdekin River sediment may thus enter Cleveland Bay 32 days y^{-1}. The model suggests that this inflow is $3.6 \times 10^8\ m^3\,d^{-1}$. Assuming that this sediment deposits in Cleveland Bay the Burdekin River may discharge about 34,500 t y^{-1} of fine sediment in Cleveland Bay.

Thus, in years with no cyclones but with river floods, fine sediment may accumulate in Cleveland Bay at a rate of 60,400 t y^{-1} (Fig. 6). A small cyclone may flush out much of this sediment in one event but the budget still remains positive, i.e. the bay fills with sediment under present land-use conditions that produce high sediment discharge from the watersheds. A fraction of that sediment accumulates in the deeper waters of the bay where tradewinds cannot resuspend it; the remaining sediment accumulates in areas where it was frequently resuspended by waves under tradewinds, thus increasing the turbidity and stressing the seagrass and corals. Indeed our data show much higher SSC over the coral reefs of Magnetic Island than those reported by Orpin et al. (2004), at values threatening the survival of these reefs (Fabricius, 2005).

5. Conclusions

A new method was proposed to parameterise wave-induced excess pore pressure build-up, so that the bed erodes both by wave-induced bed liquefaction and by excess shear stress. This formula proposed as Eqs. (7)–(10) satisfactorily reproduces the observations across a wide range of oceanographic conditions in Cleveland Bay without changing the calibrated values of the empirical coefficients A_1 and A_2.

An algorithm is needed to retrieve SSC values from MODIS data for GBR waters. Until then a quantitative comparison between predicted and MODIS observed distribution of SSC in the GBR is not possible.

Our field data fitted by Eq. (5) show that in Cleveland Bay the settling velocity w_s is a factor of 10 higher than that measured in laboratory experiments in the absence of biology (e.g. Ross, 1988). This highlights the role of the biology in enhancing the settling rate of suspended fine sediment (Ayukai and Wolanski, 1997; Wolanski et al., 1998; Lumborg et al., 2006; Wolanski, 2007; Maerz and Wirtz, 2009; Pejrup and Mikkelsen, 2010). Thus when calculating the settling flux D from Eq. (6), values of w_s from laboratory experiments where the biology is excluded cannot be used; instead only measured values of w_s in the field should be used.

The data show (Fig. 2a) that late in the dry season, fine sediment was resuspended in smaller quantities than at the beginning of the dry season under comparable wind/wave conditions. This suggests that during the dry season the sediment over the fringing reef was exported into deeper waters and that the bed in shallow reefal waters was armoured by winnowing. These findings may have ecological and management implications. Nutrients, fine sediments (mud), and agrochemicals from human activities on land degrade coastal coral reefs worldwide (Brodie et al., 2001; Wilkinson, 2004; Bellwood et al., 2004; Pandolfi et al., 2005; Richmond et al., 2007). The mechanisms responsible for this degradation are many, including shading and smothering benthic organisms by the mud, bio-eroders whose density is also controlled by the mud, and algal mats that grow over the coral, retain the mud and prevent the recruitment of coral larvae (Stamski and Field, 2006; Richmond et al., 2007). The resulting degradation depends on coral species, sedimentation rates, the residence time of this mud on the corals, and the presence of TEP (transparent exopolymer particles; Fabricius, 2005). Thus the fate of corals depends on the composition and fate of the riverine mud, and how long this mud remains near coral reefs being resuspensed by waves and degrading of coral reefs long after the river floods have ceased (Fulton and Bellwood, 2005; Richmond et al., 2007; Wolanski et al., 2008).

For management this may be the most significant finding of this study, namely that land-based remediation measures that reduce the amount of riverine fine sediment inflow into Cleveland Bay would reduce the length of time when high turbidity prevails over seagrass and corals. Order of magnitude estimates suggest that if land-care management policies were implemented in the catchments of the Ross and Burdekin rivers to reduce by a factor of 4 the fine sediment discharge, the turbidity in Cleveland Bay would be halved after 170 days following cessation of river floods, which in turn would promote seagrass and reef growth.

Acknowledgments

This project/research was supported by the Australian Government's Marine and Tropical Sciences Research Facility, implemented in North Queensland by the Reef and Rainforest Research Centre Ltd. The study was also carried out within the scope of the project "A second-generation model of the ocean system", funded by the Communauté Française de Belgique as Actions de Recherche Concertées under contract ARC 04/09-316. This work is a contribution to the development of SLIM, the Second-generation Louvain-la-Neuve Ice-ocean Model (www.climate.be/SLIM). Jonathan Lambrechts is a Research Fellow with the Belgium Fund for Research in Industry and Agriculture (FRIA).

References

Aldridge, J.N., Rees, J.M., 1997. Interpreting observations of near-bed sediment concentration and estimation of 'pick-up' function constants, pp. 289–303. In: Burt, N., Parker, R., Watts, J. (Eds.), Cohesive Sediments. John Wiley & Sons Limited, Chichester, 458 pp.

Andersen, T.J., Lanuru, M., van Bernem, C., Pejrup, M., Riethmueller, R., 2010. Erodibility of a mixed mudflat dominated by microphytobenthos and *Cerastoderma edule*, East Frisian Wadden Sea, Germany. Estuarine, Coastal and Shelf Science 87, 197–206.

Ayukai, T., Wolanski, E., 1997. Importance of biologically mediated removal of fine sediments from the Fly River plume, Papua New Guinea. Estuarine, Coastal and Shelf Science 44, 629–639.

Bainbridge, Z., Lewis, S., Brodie, J., 2007. Event-based Community Water Quality Monitoring in the Burdekin Dry Tropics Region, volume 1: 2006/07 Wet Season Report. Burdekin Solutions Ltd, Townsville, 91 pp. http://www.bdtnrm.org.au/resources/downloads/Bainbridge-et-al-2007a-Event-based-WQ-monitoring-Vol-1.pdf.

Baith, K., Lindsay, R., Fu, G., Mcclain, C.R., 2001. SeaDAS, a data analysis system for ocean-color satellite sensors. EOS, Transactions of the American Geophysical Union 82, 202.

Bellwood, D.R., Hughes, T.P., Folke, C., Nystrom, M., 2004. Confronting the coral reef crisis. Nature 429, 827–833.

Brodie, J., Christie, C., Devlin, M., Haynes, D., Morris, M., Waterhouse, J., Yorkston, H., 2001. Catchment management and the Great Barrier Reef. Water Science and Technology 43, 203–211.

Carter, R.M., Johnson, D.P., Hooper, K.G., 1993. Episodic post-glacial sea-level rise and the sedimentary evolution of a tropical continental embayment (Cleveland Bay, Great Barrier Reef shelf, Australia). Australian Journal of Earth Sciences 40, 229–255.

Chen, Z., Hu, C., Muller-Karger, F., 2007. Monitoring turbidity in Tampa Bay using MODIS/Aqua 250-m imagery. Remote Sensing of Environment 109, 207–220.

Dyer, K.R., 1986. Coastal and Estuarine Sediment Dynamics. John Wiley & Sons, Chichester, 342 pp.

Einstein, H.A., Krone, R.B., 1962. Experiments to determine modes of cohesive sediment transport in salt water. Journal of Geophysical Research 67, 1451–1462.

Fabricius, K., 2005. Effects of terrestrial runoff on the ecology and coral reefs: review and synthesis. Marine Pollution Bulletin 50, 125–146.

Foda, M.A., Huang, H.-C., 2001. A fluidization model for crossshore sediment transport by water waves. In: ASCE's Waves 2001 Conference. 2–6 September 2001, San Francisco, CA.

Fulton, C.J., Bellwood, D.R., 2005. Wave-induced water motion and the functional implications for coral reef fish assemblages. Limnology & Oceanography 50, 255–264.

Furnas, M.J., 2003. Catchments and Corals, Terrestrial Runoff to the Great Barrier Reef. Australian Institute of Marine Science, CRC Reef Research Centre, Townsville, 334 pp.

Johansen, C., Larsen, T., Petersen, O., 1997. Experiments on erosion of mud from the Danish Wadden Sea, pp. 305–314. In: Burt, N., Parker, R., Watts, J. (Eds.), Cohesive Sediments. John Wiley & Sons Limited, Chichester, 458 pp.

King, B., McAllister, F., Wolanski, E., Done, T., Spagnol, S., 2001. River plume dynamics in the central Great Barrier Reef, pp. 145–160. In: Wolanski, E. (Ed.), Oceanographic Processes of Coral Reefs: Physical and Biological Links in the Great Barrier Reef. CRC Press, Boca Raton, Florida, 356 pp.

Kuo, Y.-Y., Chiu, Y.-F., 1994. Transfer function between the wave height and wave pressure for progressive waves. Coastal Engineering 23, 81–93.

Lahet, F., Stramski, D., 2010. MODIS imagery of turbid plumes in San Diego coastal waters during rainstorm events. Remote Sensing of Environment 114, 332–344.

Lambeck, A., Woolfe, K.J., 2000. Composition and textural variability along the 10 m isobath, Great Barrier Reef: evidence for pervasive northward sediment transport. Australian Journal of Earth Sciences 47, 327–335.

Lambrechts, J., Hanert, E., Deleersnijder, E., Bernard, P.-E., Legat, V., Remacle, J.-F., Wolanski, E., 2008. A multi-scale model of the hydrodynamics of the whole Great Barrier Reef. Estuarine, Coastal and Shelf Science 79, 143–151.

Lewis, S., Bainbridge, Z., Brodie, J., 2008. Water quality monitoring of the Black Ross Basins: 2007/08 wet season. ACTFR Report No. 08/04 for the Black Ross Water Quality Improvement Plan. ACTFR, James Cook University. http://cms.jcu.edu.au/idc/groups/public/documents/technical_report/jcuprd_055221.pdf.

Liessmann, L. Lewis, S. Bainbridge, Z. Brodie, J., Faithful, J., Maughan. M., 2007. Event-based water quality monitoring of the Ross and Black River Basins during the 2006/07 wet season. ACTFR Report No. 07/09 for the Black Ross Water Quality Improvement Plan. Australian Centre for Tropical Freshwater Research, James Cook University, Townsville. http://cms.jcu.edu.au/pv_obj_cache/pv_obj_id_7CF091BF29D5569BC0DEEC45BA428F4B7ED62800/filename/jcuprd_055677.pdf.

Lou, J., Ridd, P.V., 1997. Modelling of suspended sediment transport in coastal areas under waves and currents. Estuarine, Coastal and Shelf Science 45, 1–16.

Lumborg, U., Andersen, T.J., Pejrup, M., 2006. The effect of *Hydrobia ulvae* and microphytobenthos on cohesive sediment dynamics on an intertidal mudflat described by means of numerical modelling. Estuarine, Coastal and Shelf Science 68, 208–220.

Maa, P.-Y., Mehta, A.J., 1987. Mud erosion by waves: a laboratory study. Continental Shelf Research 7, 1269–1284.

Maerz, J., Wirtz, K., 2009. Resolving physically and biologically driven suspended particulate matter dynamics in a tidal basin with a distribution-based model. Estuarine, Coastal and Shelf Science 84, 128–138.

Miller, R.L., Mckee, B.A., 2004. Using MODIS Terra 250 m imagery to map concentrations of total suspended sediment in coastal waters. Remote Sensing of Environment 93, 259–266.

Orpin, A.R., Ridd, P.V., Thomas, S., Anthony, K., Marshall, P., Oliver, J., 2004. Natural turbidity variability and weather forecasts in risk management of anthropogenic sediment discharge near sensitive environments. Marine Pollution Bulletin 49, 602–612.

Pandolfi, J.M., Jackson, J.B.C., Baron, N., Bradbury, R.H., Guzman, H.M., Hughes, T.P., Kappel, C.V., Micheli, F., Ogden, J.C., Possingham, H.P., Sala, E., 2005. Are coral reefs on the slippery slope to slime? Science 307, 1725–1726.

Partheniades, E., 1986. A fundamental framework for cohesive sediment dynamics. In: Mehta, A.J. (Ed.), Estuarine Sediment Dynamics. Lecture Notes on Coastal and Estuarine Studies 14, pp. 219–250. Chapter XII.

Pejrup, M., Mikkelsen, O.A., 2010. Factors controlling the field settling velocity of cohesive sediment in estuaries. Estuarine, Coastal and Shelf Science 87, 177–185.

Richmond, R.H., Rongo, T., Golbuu, Y., Victor, S., Idechong, N., Davis, G., Kostka, W., Neth, L., Hamnett, M., Wolanski, E., 2007. Watersheds and coral reefs: conservation science, policy and implementation. BioScience 57, 598–607.

Rodriguez, H.N., Mehta, A.J., 2000. Longshore transport of fine grained sediment. Continental Shelf Research 20, 1419–1432.

Ross, M.A., 1988. Vertical structure of estuarine fine sediment suspension. PhD thesis, University of Florida, Gainesville, 206 pp.

Sheng, Y.P., Lick, W., 1979. The transport and resuspension of sediments in a shallow lake. Journal of Geophysical Research 84 (C4), 1809–1826.

Soulsby, R.L., Hamm, L., Klopman, G., Myrhaug, D., Simons, R.R., Thomas, G.P., 1993. Wave-current interaction within and outside the bottom boundary layer. Coastal Engineering 21, 41–69.
Stamski, R.E., Field, M.E., 2006. Characterization of sediment trapped by macroalgae on a Hawaiian reef flat. Estuarine, Coastal and Shelf Science 66, 211–216.
Tsai, C.-H., Huang, M.-C., Young, F.-J., LinY, .C., Li, H.-W., 2005. On the recovery of surface wave by pressure transfer function. Ocean Engineering 32, 1247–1259.
Wang, M., Shi, W., 2007. The NIR-SWIR combined atmospheric correction approach for MODIS ocean color data processing. Optics Express 15, 15722–15733.
Wilkinson, C., 2004. Status of Coral Reefs of the World: 2004, vols. 1 and 2. Australian Institute of Marine Science, Townsville, 557 pp.
Winterwerp, J.C., van Kesteren, W.G.M., 2004. Introduction to the physics of cohesive sediments in the marine environment. In: Developments in Sedimentology, vol. 56. Elsevier, Amsterdam.
Wolanski, E., Gibbs, R., Ridd, P., Mehta, A., 1992. Settling of ocean-dumped dredged material, Townsville, Australia. Estuarine, Coastal and Shelf Science 35, 473–490.
Wolanski, E., King, B., Galloway, D., 1995. The dynamics of the turbidity maximum in the Fly River estuary, Papua New Guinea. Estuarine, Coastal and Shelf Science 40, 321–338.
Wolanski, E., Spagnol, S., Ayukai, T., 1998. Field and model studies of the fate of particulate carbon in mangrove-fringed Hinchinbrook Channel, Australia. Mangroves and Salt Marshes 2, 205–221.
Wolanski, E., Spagnol, S., 2003. Dynamics of the turbidity maximum in King Sound, tropical Western Australia. Estuarine, Coastal and Shelf Science 56, 877–890.
Wolanski, E., 2007. Estuarine Ecohydrology. Elsevier, Amsterdam, 157 pp.
Wolanski, E., Fabricius, K., Cooper, T., Humphrey, C., 2008. Wet season fine sediment dynamics on the inner shelf of the Great Barrier Reef. Estuarine, Coastal and Shelf Science 77, 755–762.
Zhang, M., Tang, J., Dong, Q., Song, Q., Ding, J., 2010. Retrieval of total suspended matter concentration in the Yellow and East China Seas from MODIS imagery. Remote Sensing of Environment 114, 392–403.